frontiers | Frontiers in Astronomy and Space Sciences

TYPE Perspective
PUBLISHED 12 October 2022
DOI 10.3389/fspas.2022.1026455

OPEN ACCESS

EDITED BY
Alexa Jean Halford,
Goddard Space Flight Center (NASA),
United States

REVIEWED BY
Alexey A. Kuznetsov,
Institute of Solar-Terrestrial Physics
(RAS), Russia

*CORRESPONDENCE
Jason E. Kooi,
jason.kooi@nrl.navy.mil

SPECIALTY SECTION
This article was submitted to Space
Physics,
a section of the journal
Frontiers in Astronomy and Space
Sciences

RECEIVED 23 August 2022
ACCEPTED 26 September 2022
PUBLISHED 12 October 2022

CITATION
Carson G, Kooi JE, Helmboldt JF,
Markowski BB, Bonanno DJ and
Hicks BC (2022), DLITE—An
inexpensive, deployable interferometer
for solar radio burst observations.
Front. Astron. Space Sci. 9:1026455.
doi: 10.3389/fspas.2022.1026455

DLITE—An inexpensive, deployable interferometer for solar radio burst observations

George Carson[1], Jason E. Kooi[2]*, Joseph F. Helmboldt[2], Blerta B. Markowski[2], David J. Bonanno[2] and Brian C. Hicks[2]

[1]Department of Physics and Astronomy, Dickinson College, Carlisle, PA, United States, [2]United States Naval Research Laboratory, Washington, DC, United States

Solar radio bursts (SRBs) are brief periods of enhanced radio emission from the Sun. SRBs can provide unique insights into the plasma structure where emission occurs. SRBs can also provide critical information concerning space weather events such as coronal mass ejections or solar energetic particle events. Providing continuous monitoring of SRBs requires a full network of detectors continuously monitoring the Sun. A promising new network is being developed, employing a four-element interferometer called the Deployable Low-band Ionosphere and Transient Experiment (DLITE) array. DLITE, which operates in a 30–40 MHz band, was specifically designed to probe the Earth's ionosphere using high resolution measurements (1.024-s temporal resolution, 16.276-kHz frequency resolution); however, this also makes DLITE a powerful new tool for providing detailed observations of SRBs at these frequencies. DLITE is particularly adept at detecting long-duration SRBs like Type II and Type IV bursts. DLITE provides high resolution SRB data that can complement ground-based networks like e-Callisto or space-based observations, e.g., from *Wind*/WAVES. As an inexpensive interferometer, DLITE has strong potential as an educational tool: DLITE can be used to study the ionosphere, SRBs, and even Jovian radio bursts. Future DLITE arrays could be enhanced by using the full 20–80 MHz band accessible by the antennas and employing its millisecond time-resolution capability; this would improve DLITE's ability to track long-duration bursts, create the opportunity to study short-duration Type III bursts in detail, and, in particular, make the study of Type I bursts practical.

KEYWORDS

solar corona, solar radio bursts, coronal plasma density, coronal mass ejection, radio astronomy

1 Introduction

Solar radio bursts (SRBs) are brief periods of enhanced radio emission from the Sun. This enhancement can range from just above background levels to orders of magnitude more. SRBs can also be associated with major solar activity, such as solar flares and coronal mass ejections (CMEs). SRBs were first observed during the 1940s (e.g. Allen,

1947; Payne-Scott et al., 1947) and categorized into separate types based on their temporal and spectral structure: initially Types I, II, and III (Wild and McCready, 1950); then Types I, II, III, IV-stationary, IV-moving, and V (Wild et al., 1963); and, later, many more specialized types, such as "herringbones" (Cairns and Robinson, 1987; Cane and White, 1989; Carley et al., 2015) and solar S bursts (McConnell, 1983; Morosan et al., 2015).

SRBs are typically detected by low frequency (< 100s of MHz) radio instruments and typically decrease in frequency as a function of time. This is a consequence of the emission mechanism. Many radio bursts result from plasma emission (at either the fundamental and/or harmonic frequency), which occurs when a disturbed plasma's electrons are displaced relative to the ions and experience a restoring force (i.e. the Coulomb force), causing them to oscillate. The fundamental electron plasma frequency is given by

$$f_{\mathrm{pe}} = \frac{1}{2\pi}\sqrt{\frac{e^2 n_{\mathrm{e}}}{\epsilon_0 m_{\mathrm{e}}}} \approx 8980\sqrt{n_{\mathrm{e}}} \qquad [\mathrm{Hz}] \qquad (1)$$

where e, ϵ_0, and m_{e} are the electron charge, permittivity of free space, and mass of an electron, respectively, and the plasma density, n_{e}, is given in cm^{-3}; plasma densities in the range 10^6–$10^9\,\mathrm{cm}^{-3}$ correspond to radio frequencies of $\approx 10-300$ MHz.

As Eq. 1 demonstrates, SRBs directly provide n_{e} information. SRBs also provide unique insights into the plasma structure and coronal height where emission occurs because the coronal n_{e} is determined by region (i.e. coronal hole, streamer, *etc.*) and heliocentric distance. The type of SRB can provide information concerning different physical processes involved in space weather events such as CMEs or solar energetic particle (SEP) events.

Type I bursts are very fast ($\lesssim 1$ s) and tend to occur in "noise storms." Type I bursts are typically observed at frequencies of 50–300 MHz (Dulk, 1985). Type I storms can indicate energetic processes within closed magnetic loops rising high into the corona, as suggested by their emission predominantly occurring below 300 MHz (e.g. see Vourlidas, 2004; Vourlidas et al., 2020). Because Type I storms usually arise from loop systems above active regions with strong magnetic fields and are associated with flux emergence, they may act as a precursor to the eruption of some CMEs.

Type II bursts are relatively long ($\gtrsim 10$ min) and typically emit at both the fundamental and harmonic frequencies. Type II are associated with plasma shocks and, therefore, frequently observed when a CME erupts and generates a shock front. Type II bursts cover a broad range in frequencies, corresponding to the shock propagating outward and encountering more tenuous plasma. The frequency drift rate is ≈ -0.1 to -0.4 MHz s^{-1}, where the negative sign represents a decrease in frequency over time (Carley et al., 2020; Miteva et al., 2022). Both the fundamental and harmonic bands can each "split" into upper and lower bands; the frequency difference between the upper and lower bands is associated with the shock-compression ratio and, therefore, provides an estimate for the Alfvén Mach number that can be used to estimate the coronal magnetic field strength local to the shock (Vršnak et al., 2004; Gopalswamy et al., 2012; Kumari et al., 2017; Mahrous et al., 2018).

Type III bursts are fast (~ few seconds) and can also emit at both fundamental and harmonic frequencies. These are associated with electron beams propagating outward into the corona, typically along open magnetic field lines. Similar to Type II bursts, these decrease in frequency as the electron beams move through coronal plasma with decreasing background electron densities. The frequency drift rate is much larger than Type II bursts, varying from several MHz s^{-1} to $\lesssim 100$ MHz s^{-1} (Reid, 2020; Miteva et al., 2022). The dynamics of Type III bursts can give insights into the evolution of coronal structures like flux tubes. McCauley et al. (2017) used the Murchison Widefield Array (MWA; Li et al., 2018) to perform spectroscopic imaging of a series of Type III bursts, tracking them over several frequencies to illustrate their evolution from a single source in the inner corona to two separate sources split between two separate flux tubes. Type III bursts can also provide insights into SEP events (Klein, 2021) because of their association with escaping electron beams.

Type IV bursts are often categorized as "stationary" or "moving" based on their spatial characteristics. Type IV-stationary bursts can last from tens of minutes to several hours, remaining relatively constant in frequency; consequently, the emission region is believed to be stationary within the corona. Type IV-moving bursts can last for several 10 s of minutes, slowly decreasing in frequency, and are generally attributed to energetic electrons trapped inside a CME. They can emit through a number of mechanisms, but if the emission mechanism can be identified, then Type IV-moving bursts can provide unique insights into the CME. For instance, detecting gyrosynchrotron radio emission and measuring the circular polarization provides information concerning the CME's magnetic field strength as well as the nonthermal particle distribution interacting with the CME's magnetic field (Gopalswamy and Kundu, 1987; Bastian et al., 2001; Sasikumar Raja et al., 2014; Mondal et al., 2020).

Table 1 in Dulk (1985) provides a historical overview of SRB characteristics and Table 1 in Vourlidas et al. (2020) sums up some of the parameters of SRBs (as well as other radio phenomena such as Faraday rotation) and their relevance for space weather research. In particular, Vourlidas et al. (2020) describe several paths forward for SRB science, including development of large sample analyses of Type I storms and Type IV-moving bursts with a focus on deriving magnetic fields for CMEs from the latter; this requires continuous monitoring of SRBs. Here, we will discuss low-cost methods for low-frequency monitoring and characterization of SRBs with an overview in

Section 2, a description of the DLITE system's solar monitoring capabilities in Section 3, and discussion in Section 4.

2 Inexpensive, deployable SRB detectors

Over the last decade, new instruments such as the Low Frequency Array (LOFAR; van Haarlem et al., 2013), Karl G. Jansky Very Large Array (VLA; Perley et al., 2011), Mingantu Ultrawide Spectral Radioheliograph (MUSER; Yan et al., 2016), Expanded Owens Valley Solar Array (EOVSA; Gary et al., 2018), Long Wavelength Array (LWA; Taylor et al., 2012), and MWA have provided detailed new insights into SRBs. Some of these facilities (e.g. LOFAR and the VLA), however, are not solar-dedicated instruments, but competitive PI-driven instruments that only perform solar observations sporadically. All of these facilities (and other likes them), though, share a common flaw: they are expensive, "permanent" facilities, each wholly unique in design and construction.

Providing continuous monitoring of SRBs typically requires a full network of detectors, each continuously monitoring the Sun. One such network is e-Callisto (Benz et al., 2005). Originally consisting of two spectrometers located in ETH Zurich radio observatory in Bleien (Switzerland) and one at the National Radio Astronomy Observatory in Green Bank (United States), the Compact Astronomical Low-frequency, Low-cost Instrument for Spectroscopy in Transportable Observatories (CALLISTO) has expanded into a large network of spectrometers located around the world.

Another instructional example is the Deployable Low-band Ionosphere and Transient Experiment (DLITE; Helmboldt et al., 2021) array. DLITE is a low-cost, four-element interferometer created as an inexpensive alternative to larger, permanent interferometers (e.g. the VLA or LWA). Each of the four antennas is an LWA antenna (for detailed descriptions, see Hicks et al., 2012), operating in a 30–40 MHz band, but with good sensitivity (sky-noise dominated) in the 20–80 MHz range. DLITE arrays were specifically designed to probe the Earth's ionosphere, hence their narrow band centered on 35 MHz. They continuously monitor the brightest cosmic radio sources to characterize ionospheric structure and have been used to study km-scale irregularities at mid-latitudes and medium-scale Traveling Ionospheric Disturbances (Helmboldt and Zabotin, 2022) as well as mid-latitude ionospheric magnetic field fluctuations (Helmboldt et al., 2022). Software used to run the system and perform analysis has been written in Python using GNURadio (https://www.gnuradio.org), NumPy (https://numpy.org), SciPy (https://scipy.org), and Astropy (https://www.astropy.org). This software is currently available at https://github.com/USNavalResearchLaboratory/DLITE.

Individual sources are resolved from one another via time difference of arrival (TDOA) (i.e., bandwidth smearing), requiring a relatively large fractional bandwidth (~20% or more). Consequently, the default mode for the correlator only outputs two polarization products, XX and YY (X is the north/south feed, Y is east/west). Outputting all four products (XX, YY, XY, and YX) requires a reduction in bandwidth so that the CPU can keep up with twice the number of correlations (typically from 8.33 MHz to 6.25 MHz). However, this mode has been used on occasion when polarimetry was needed, e.g., for an observation of a Jupiter burst presented by Helmboldt et al. (2021). In this case, the burst was shown to be fully right-hand circularly polarized as expected, which confirmed the polarization capabilities of the system. Thus, for dedicated solar observations, this reduced bandwidth, full polarization mode is likely more optimal.

To track apparent motions caused by ionospheric density gradients, interferometric images are made around each bright source with a resolution of ~1–1.5°. Due to the extremely sparse nature of the array, the synthesized beam has large sidelobes relatively close to the main lobe (~3° away). However, this is significantly smaller than the typical ionospheric position offsets ($\lesssim$ 0.3°). This is why the isolation of sources via TDOA/bandwidth smearing is crucial so that sidelobes from other sources have minimal impact on these images. While the resolution within such images is not good enough for detailed imaging of solar bursts, in principal, they could be used to estimate the location of the dominant emission. However, this would require a grid of sources with fixed positions that are within the ionospheric isoplanatic patch around the Sun on the sky to get an absolute position free from ionospheric effects. This can be done quite effectively with larger, more sensitive telescopes (Chhabra et al., 2021). However, the 35-MHz isoplanatic patch at mid-latitudes is usually $\lesssim$ 5° (Kassim et al., 2007), and the bright sources detectable with DLITE are spaced from one another by 36°–150° on the sky. Thus, locating the source of solar burst emission with DLITE imaging is not possible in practice.

Three DLITE arrays have been established, shown as blue circles in Figure 1A: one located near LWA station 1 (LWA-1) in New Mexico (DLITE-NM), one located near Pomonkey, Maryland (DLITE-POM), and one located in Florida (DLITE-FL). There is another DLITE array currently being constructed in Texas that will be online in the near future (red circle) and several other locations have also been proposed (orange circles). Because DLITE arrays were principally designed as probes of ionospheric structures, they return high resolution data (1.024-s temporal resolution, 16.276-kHz frequency resolution) allowing for sensitive measurements of SRBs.

3 DLITE as an SRB detector

DLITE is designed to study the ionosphere; however, at 30–40 MHz, SRBs are the strongest source of radio emission in the sky. This frequency range corresponds roughly to emission

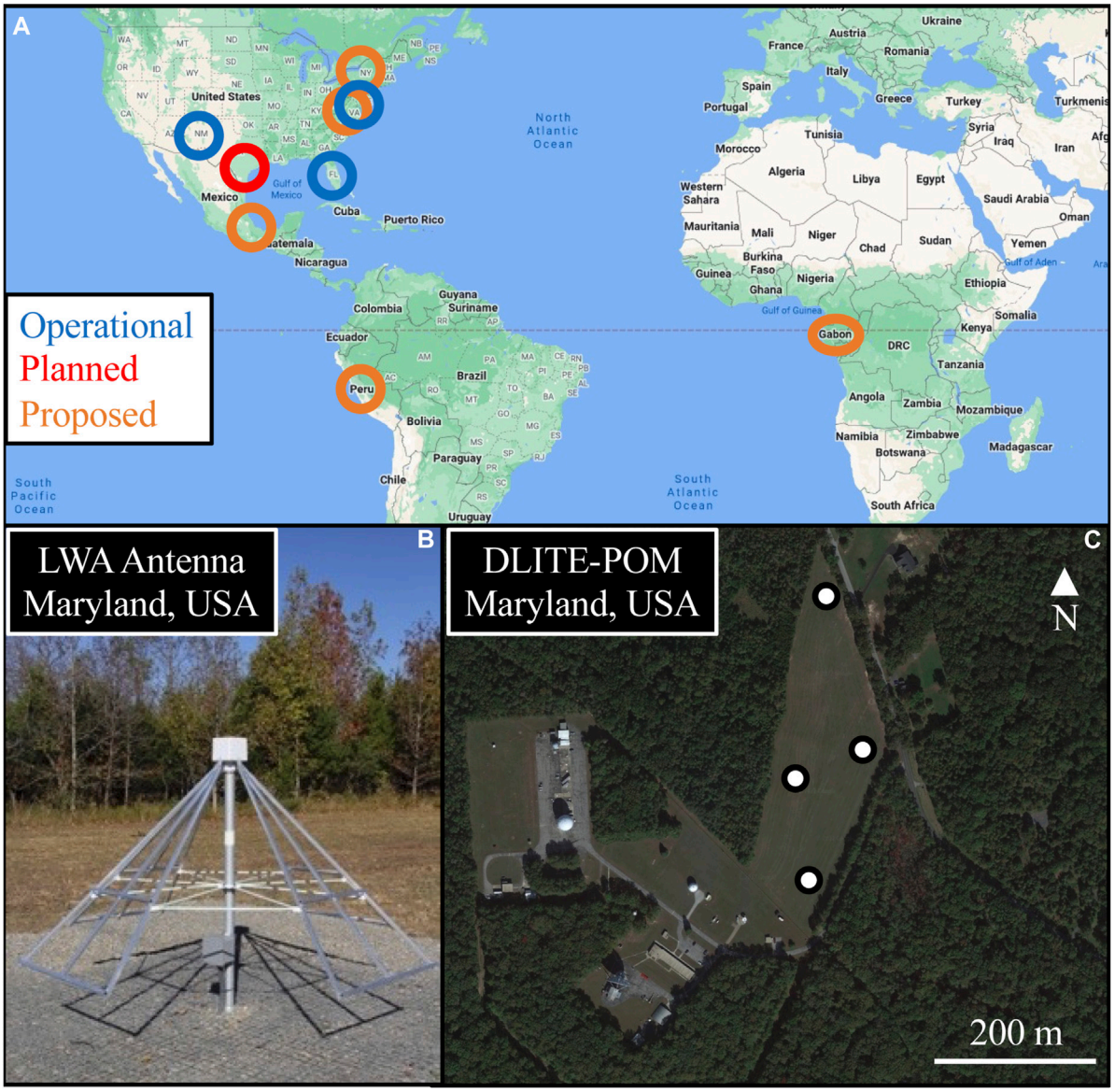

FIGURE 1
An illustrative example of a deployable radio array is the Deployable Low-band Ionosphere and Transient Experiment (DLITE) array. **(A)** shows the locations of three operational DLITE arrays (blue), one planned array (red), and five proposed arrays (orange) around the world. **(B)** displays a Long Wavelength Array (LWA) antenna as it appears on-site at the DLITE-POM station in Maryland, United States. **(C)** provides an overhead view of the DLITE-POM site; the four antenna positions are given by the white plotted points.

located at heliocentric distances of 2–3 $R_\odot$ and makes DLITE observations of SRBs quite complementary to other instruments. Many ground-based SRB detectors operate near or well above these frequencies because the ionosphere limits their utility below DLITE frequencies. Many space-based SRB detectors (e.g. *Wind*/WAVES Bougeret et al., 1995) operate near or below these frequencies because they are located well beyond Earth's ionosphere. An instructive table of SRB detectors can be found in Table 1 of Miteva et al. (2022).

DLITE's primary strength as a SRB detector is its sensitivity. As an interferometer, DLITE provides an opportunity to study the properties of SRBs in more detail than single-antenna detectors given the high signal-to-noise ratio (SNR). This is achieved through a quantity known as the bispectrum, which combines the antenna visibilities from each unique triangle/triple within the array such that the phase of the resulting complex quantity is the so-called "closure phase." For antennas *i*, *j*, and *k* in the antenna triple, the bispectrum is given by

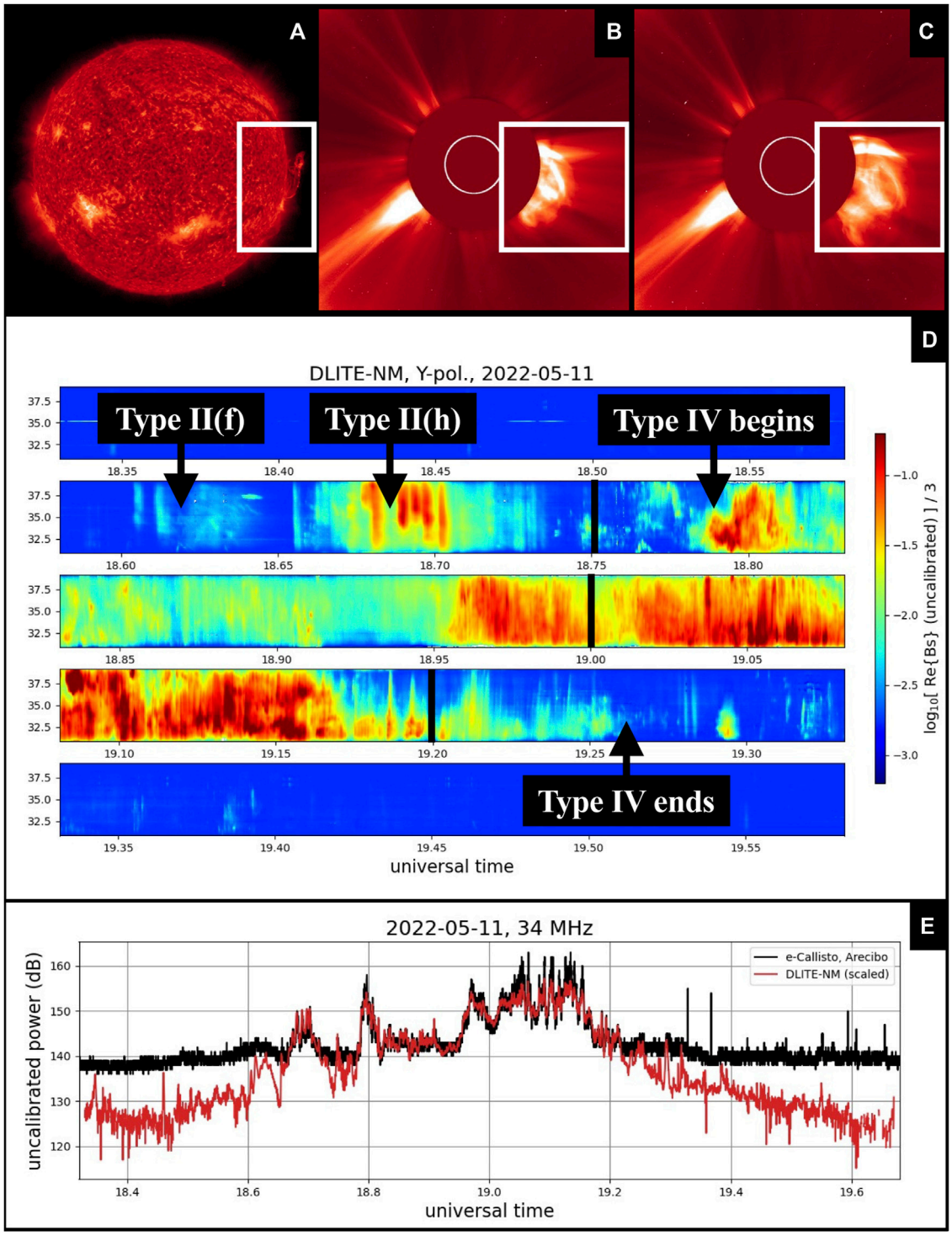

FIGURE 2
A series of high-resolution radio bursts associated with a CME seen by DLITE arrays on 2022 May 11. **(A)** *SDO*/AIA 304 Å image of the emerging CME at 18:45 UT, shortly after the CME erupted at 18:30 UT. **(B)** and **(C)** *SOHO*/LASCO-C2 coronagraph images of the CME erupting at 19:00 UT and 19:12 UT, respectively. The white boxes highlight the position of the CME. **(D)** DLITE-NM detection of SRBs with black vertical bars corresponding to the times associated with panels **(A)–(C)**. Arrows indicate the Type II fundamental and harmonic (Type II(f) and Type II(h), respectively) SRBs as well as the beginning and end of the Type IV-moving SRB. **(E)** Time series of the SRBs near the designated radio astronomy band at 34 MHz from the e-Callisto spectrometer at Arecibo Observatory (black) with a scaled version of the DLITE-NM bispectrum at the same frequency (red).

$$Bs \equiv V_{i,j} V^*_{i,k} V_{j,k} \quad (2)$$

where $V_{i,j}$ is the complex visibility between antennas i and j and * denotes the complex conjugate. This appears as Eq. 15 in Helmboldt et al. (2021).

The key characteristic of the bispectrum is that antenna-based phase errors sum to zero as does the phase contribution from a single, dominant point-like source (this is why, e.g., the closure phase forms the basis for self-calibration methods in interferometric imaging applications). For four antennas, the ratio of the SNR of the bispectrum averaged over all four unique triples to that of a spectrum incoherently averaged from four antennas recorded separately is $s^2/2$, where s is the SNR for a single baseline (Law and Bower, 2012). Provided $s > \sqrt{2}$, the SNR for the bispectrum increases rapidly with s; consequently, the bispectrum provides the ability to search for bright transient sources like SRBs on short time scales without requiring all-sky maps.

At the nominal DLITE frequency of 35 MHz, the LWA antenna system equivalent flux density (SEFD) is approximately 4×10^6 Jy (Helmboldt et al., 2021). For the default setup of 1.024-s integration times and frequency channel widths of 16.276 kHz, $s \simeq 3 \times 10^4$. According to Law and Bower (2012), for a four-element system like DLITE with four unique triples, a mean bispectrum signal-to-noise ratio of three or greater requires $s > 1.44$, or a source that is at least 4.4×10^4 Jy. This is supported by the fact that when Cassiopeia A and Cygnus A are both visible, fringe patterns are often visible within DLITE bispectra due to the combination of the two sources. Conversely, neither source is detected when it is above the horizon, and the other is below. Both sources are approximately 2.2×10^4 Jy (Baars et al., 1977; Helmboldt and Kassim, 2009), which is consistent with their combined fringe pattern being detected while each individual source is not.

While DLITE arrays have detected 100 s of SRBs since the first two stations came online in the fall of 2019, they are particularly adept at detecting long duration SRBs like Type II and Type IV. Figure 2 shows a series of Type II and Type IV-moving SRBs coinciding with the eruption of a CME off the western limb on 2022 May 11. The CME erupted near 18:30 UT, accompanied by an M-class X-ray flare. Figure 2A shows a 304 Å image of the CME at 18:45 UT, shortly after eruption, taken with the Atmospheric Imaging Assembly (AIA; Lemen et al., 2012) on board the *Solar Dynamics Observatory* (*SDO*; Pesnell et al., 2012). The *SDO*/AIA uses extreme ultraviolet emission to trace the flow of hot plasma as it flows along, e.g., magnetic field lines. The region in Figure 2A highlighted by the white box rapidly evolves over a period of minutes as the low corona reorganizes in response to the CME release.

Figures 2B, C show the emergence of the CME into the middle corona (e.g. 1.5–6.0 $R_\odot$, as defined in Seaton et al., 2020; West et al., 2022) at 19:00 UT and 19:12 UT, respectively, in white-light coronagraph images from the C2 Large Angle and Spectrometric Coronagraph (LASCO; Brueckner et al., 1995) on board the *Solar and Heliospheric Observatory* (*SOHO*; Domingo et al., 1995). These white-light images correspond to photospheric light Thomson-scattered off the electron plasma in the corona; consequently, features that appear "bright" correspond to very dense plasma (e.g. the coronal streamer off the eastern limb and the outer loop of the CME) and features that appear "dim" correspond to very tenuous plasma (e.g. the polar coronal holes associated with open magnetic field lines). The CME shock front is first visible at the inner edge of the *SOHO*/LASCO-C2 images at 18:36 UT.

Figure 2D shows the bispectrum for the DLITE-NM station. Vertical black bars have been placed in Figure 2D to highlight the time of each event shown in Figures 2A–C. Both the fundamental and harmonic Type II bursts are present shortly after 18:36 UT, when the shock front enters the *SOHO*/LASCO-C2 field of view. This is then followed by a long-duration Type IV-moving burst. All three DLITE stations detected these bursts. The bispectra for DLITE-POM and DLITE-FL appear in the Supplementary Material. There are small, but distinct differences among the bispectra from the three DLITE arrays. This may be a geometric effect resulting from the position of the SRB emission region in relation to the different DLITE array locations; if true, a DLITE station in Africa would demonstrate a more striking difference than those between DLITE-POM and DLITE-NM. Another possibility is that the emission region is not point-like or there are multiple emission regions and, therefore, the bispectrum response is different for each array given their different configurations. In this case, there is likely information lurking within the bispectra and/or closure phases concerning the structure of the emission region(s). These differences may also be a direct result from the ionosphere. There are times when ionospheric scintillations are strong enough to alter the spectrum of a source, but these are relatively rare at mid-latitudes. There were no indications within the DLITE data that there were strong scintillations present prior to the SRBs, and so it is unlikely that the ionosphere is the main culprit. However, we cannot rule out some ionospheric contribution to the differences observed between DLITE stations.

These radio bursts were also observed by e-Callisto stations, with the strongest detections provided by the HAARP location in Alaska (United States) and the Arecibo Observatory in Puerto Rico (United States), which both use LWA antennas for SRB detection. This offers both confirmation of the DLITE detections and also an opportunity to demonstrate the sensitivity of the DLITE bispectrum approach. In the Figure 2E, we have plotted a time series of the (uncalibrated) received power from the Arecibo e-Callisto spectrometer near the radio astronomy band at 34 MHz (in black), which is recorded at 1-s cadence, similar to DLITE. For comparison, we have also plotted the mean bispectrum from DLITE-NM at the same frequency. To compare with the Arecibo power measurement, we have

plotted $10\log_{10}(\mathrm{Re}\{Bs\})/3$, shifted up by 153 dB to best match the power during the burst.

One can see that there are several features within the DLITE-NM time series not visible within the Arecibo curve, especially around 18.75 UT and after 19.2 UT. It is also evident that the equivalent noise floor from the DLITE-NM bispectrum is at least 10 dB below that of the Arecibo curve. Since the Arecibo spectrometer uses an LWA antenna, if the DLITE-NM bispectrum was the equivalent of spectra from four antennas averaged incoherently, we would expect the noise floor to only be about 3 dB lower (i.e., a factor of $\sqrt{4}$ smaller). This lends further credence to the claims made above regarding the enhancement in sensitivity afforded by the DLITE-based bispectrum approach.

4 Discussion

The two primary advantages of ground-based SRB detectors such as CALLISTO spectrometers or DLITE arrays are that they are inexpensive to build and install, and, perhaps more importantly, they are deployable virtually anywhere. e-Callisto has found great success building a network of SRB detectors around the world, at locations ranging from major observatories to colleges. DLITE, too, is becoming more popular, with a fourth station planned in Texas (United States) in coordination with the University of Texas Rio Grande Valley (UTRGV) and several more being proposed (e.g. Figure 1). The cost for parts of a DLITE array is ≈ $45, 000 (Helmboldt et al., 2021), making it an ideal candidate for hands-on learning at universities interested in implementing their own SRB detector.

A truly unique aspect of DLITE is its multi-functional nature. It was designed to study the ionosphere; consequently, it has to be simple to deploy so DLITE stations can be placed in different geographical locations to study different regions of the ionosphere as well as a broad range of ionospheric phenomena. However, DLITE makes an excellent SRB detector precisely because it is designed to provide high time- and frequency-resolution measurements of the ionosphere. DLITE can also detect Jovian bursts when Jupiter interacts with its moon Io. While these bursts are typically confined to decametric wavelengths, they can still reach frequencies within DLITE's 30–40 MHz bandwidth. They can contain more temporal and frequency structure than SRBs, consisting of several series of short (ms-scale) bursts (e.g. Clarke et al., 2014). Similar to SRBs enhancing the Sun's radio emission, Jovian bursts make Jupiter the brightest radio source in the sky at these frequencies and, therefore, Jovian bursts can be studied using the same bispectrum approach outlined in Section 3 (see Helmboldt et al., 2021, for an example).

One of the more interesting advances in SRB research has been developing the capability to track the position of Type III bursts as the electron beams associated with them propagate outward into the corona (McCauley et al., 2017). While DLITE arrays are not capable of performing imaging spectroscopy with the precision of the MWA, an intriguing possibility is DLITE triangulation: with enough DLITE arrays located around the world, it may be possible to use their high temporal and frequency resolution to triangulate the positions of SRBs and track their progression as a function of heliocentric distance. This would be particularly useful for Type IV-moving bursts originating from electrons trapped within a CME because this distance information, supplemented with EUV or white-light imaging, could provide the approximate location of the region of emission within the CME. If the emission mechanism for a given Type IV-moving burst is, e.g., gyrosynchrotron, then the magnetic field strength can be determined and localized within the CME *via* triangulation.

Facilitating triangulation would require testing new observing modes with much higher temporal resolution. As an example, DLITE-NM and DLITE-POM are about 2,800 km apart, implying a maximum delay of 9.3 ms; consequently, generating bispectra with a sampling interval of ~ 1 ms would be sufficient given the high SNR of SRBs. This would increase the data output by three orders of magnitude and, therefore, it is not feasible to make this the default observing mode. An effective trigger would need to be developed to initiate this high time resolution mode. The DLITE arrays are synchronized to GPS time (accurate within $\lesssim 30$ ns), which should be sufficient for performing relative timing of features within the bispectra.

While these DLITE bispectra showcase highly detailed temporal and spectral structure within the SRBs, the narrow bandwidth can make full identification and analysis of SRBs difficult; however, these DLITE data can be supplemented by ground-based data from the e-Callisto network or space-based data from, e.g., the *Wind*/WAVES instrument, which mitigates this limitation in the case of Type III bursts because they emit over a broad range in frequencies. In addition, the two linear polarization feeds for each DLITE antenna can be tuned to separate frequencies. This can be used to effectively double the available bandwidth at the expense of polarization information. This dual frequency mode is also being explored for the study of km-scale ionospheric irregularities that cause scintillations at DLITE frequencies and, thus, may become a standardized observing mode in the near future.

The study of Type I bursts, though, is restricted by the narrow bandwidth as well as the integration time for the DLITE correlator (≈ 1.024 s). The narrow DLITE band is just below the frequency band over which Type I bursts typically occur (e.g. 50–300 MHz Dulk, 1985). Also, individual Type I bursts occur on time scales of $\lesssim$ 1 s; consequently, the temporal resolution of DLITE is insufficient to study these bursts in detail. Fortunately, the DLITE array is very versatile. The LWA antennas used in DLITE arrays have good sensitivity over the full 20–80 MHz range. Future DLITE stations could be designed to take advantage of more of the available bandwidth, which would (1) put them within the low end of the frequency range of Type I SRBs and (2) provide more bandwidth to

make SRB identification straightforward for fast events like Type III bursts. Further, the DLITE correlator integration time can be set as low as the ratio of the number of frequency channels to the bandwidth; therefore, DLITE is capable of resolving SRB structure down to ms-scales (this is how DLITE is able to observe Jovian bursts). Using the full 20–80 MHz band with a temporal resolution on ms-scales could make DLITE a powerful new tool for studying Type I bursts and storms, as well as provide a way to study the structure of long-duration Type II or Type IV SRBs on smaller time scales.

DLITE also has strong potential as an educational tool. The inexpensive cost and scientific versatility of DLITE make it an ideal array for colleges and universities to incorporate into their facilities. This would provide students:

- excellent hands-on experience building and testing a low-frequency radio interferometer;
- the opportunity to study a broad range of science targets (e.g. ionospheric disturbances, SRBs, and Jovian bursts); and
- the chance to develop professional collaborations as students' efforts contribute to an ever-expanding network of DLITE arrays.

Reaching out to universities, especially historically black colleges or universities (HBCU) and minority-serving institutions (MI), should be an integral part of the strategy to expand the network of DLITE arrays. Similarly, countries that are developing new space programs, space weather centers, or radio astronomy programs should find value in DLITE precisely because it provides low-cost access to space and can be used to study space weather events themselves (e.g. SRBs and their association with CMEs and SEPs) as well as the effects of space weather events here at Earth (e.g. ionospheric disturbances). For example, Gabon's Agency of Space Studies and Observations (AGEOS) is currently pursuing a DLITE array installation at their facility near Libreville (see Figure 1).

Data availability statement

The datasets presented in this study can be found in online repositories. The names of the repository/repositories and accession number(s) can be found below: Long Wavelength Array data archive https://lda10g.alliance.unm.edu/~dlite/.

Author contributions

GC was responsible for the organization of this article and contributed to all sections. JK was also responsible for the article's organization and made contributions to Sections 2 through 4. JH made contributions to Sections 3 and 4. BM, DB, and BH all contributed to Sections 2 and 3.

Funding

Basic research at the United States Naval Research Laboratory (NRL) is supported by 6.1 Base funding. Development and testing of the DLITE system were supported by the Defense Advanced Research Projects Agency (DARPA) Space Environment Exploitation (SEE) program. Student research was supported by the Naval Research Enterprise Internship Program (NREIP) under the Office of Naval Research (ONR) contract N00014-21-D-4002.

Acknowledgments

The authors wish to thank the reviewer for their thoughtful comments, which improved the overall quality of this work. Derived DLITE data products are made available through the LWA data archive at https://lda10g.alliance.unm.edu/dlite/. Data from the e-Callisto network are available at http://www.e-callisto.org. The *SDO*/AIA data used here are courtesy of NASA/*SDO* and the AIA, EVE, and HMI science teams. The *SOHO*/LASCO data used here are produced by a consortium of the Naval Research Laboratory (United States), Max-Planck-Institut fuer Aeronomie (Germany), Laboratoire d'Astronomie (France), and the University of Birmingham (United Kingdom). *SOHO* is a project of international cooperation between ESA and NASA.

Conflict of interest

The authors declare that the research was conducted in the absence of any commercial or financial relationships that could be construed as a potential conflict of interest.

Publisher's note

Supplementary material

The Supplementary Material for this article can be found online at: https://www.frontiersin.org/articles/10.3389/fspas.2022.1026455/full#supplementary-material

References

Allen, C. W. (1947). Solar radio-noise of 200 Mc./s. And its relation to solar observations. *Mon. Not. R. Astron. Soc.* 107, 386–396. doi:10.1093/mnras/107.4.386

Baars, J. W. M., Genzel, R., Pauliny-Toth, I. I. K., and Witzel, A. (1977). The absolute spectrum of cas A: An accurate flux density scale and a set of secondary calibrators. *Astron. Astrophys.* 61, 99–106.

Bastian, T. S., Pick, M., Kerdraon, A., Maia, D., and Vourlidas, A. (2001). The coronal mass ejection of 1998 april 20: Direct imaging at radio wavelengths. *Astrophys. J.* 558, L65–L69. doi:10.1086/323421

Benz, A. O., Monstein, C., and Meyer, H. (2005). Callisto A new concept for solar radio spectrometers. *Sol. Phys.* 226, 143–151. doi:10.1007/s11207-005-5688-9

Bougeret, J. L., Kaiser, M. L., Kellogg, P. J., Manning, R., Goetz, K., Monson, S. J., et al. (1995). Waves: The radio and plasma wave investigation on the Wind spacecraft. *Space Sci. Rev.* 71, 231–263. doi:10.1007/BF00751331

Brueckner, G. E., Howard, R. A., Koomen, M. J., Korendyke, C. M., Michels, D. J., Moses, J. D., et al. (1995). The large Angle spectroscopic coronagraph (LASCO). *Sol. Phys.* 162, 357–402. doi:10.1007/BF00733434

Cairns, I. H., and Robinson, R. D. (1987). Herringbone bursts associated with type II solar radio emission. *Sol. Phys.* 111, 365–383. doi:10.1007/BF00148526

Cane, H. V., and White, S. M. (1989). On the source conditions for herringbone structure in type-II solar radio bursts. *Sol. Phys.* 120, 137–144. doi:10.1007/BF00148539

Carley, E. P., Reid, H., Vilmer, N., and Gallagher, P. T. (2015). Low frequency radio observations of bi-directional electron beams in the solar corona. *Astron. Astrophys.* 581, A100. doi:10.1051/0004-6361/201526251

Carley, E. P., Vilmer, N., and Vourlidas, A. (2020). Radio observations of coronal mass ejection initiation and development in the low solar corona. *Front. Astron. Space Sci.* 7, 79. doi:10.3389/fspas.2020.551558

Chhabra, S., Gary, D. E., Hallinan, G., Anderson, M. M., Chen, B., Greenhill, L. J., et al. (2021). Imaging spectroscopy of CME-associated solar radio bursts using OVRO-LWA. *Astrophys. J.* 906, 132. doi:10.3847/1538-4357/abc94b

Clarke, T. E., Higgins, C. A., Skarda, J., Imai, K., Imai, M., Reyes, F., et al. (2014). Probing Jovian decametric emission with the long wavelength array station 1. *J. Geophys. Res. Space Phys.* 119, 9508–9526. doi:10.1002/2014JA020289

Domingo, V., Fleck, B., and Poland, A. I. (1995). The SOHO mission: An overview. *Sol. Phys.* 162, 1–37. doi:10.1007/BF00733425

Dulk, G. A. (1985). Radio emission from the sun and stars. *Annu. Rev. Astron. Astrophys.* 23, 169–224. doi:10.1146/annurev.aa.23.090185.001125

Gary, D. E., Chen, B., Dennis, B. R., Fleishman, G. D., Hurford, G. J., Krucker, S., et al. (2018). Microwave and hard X-ray observations of the 2017 september 10 solar limb flare. *Astrophys. J.* 863, 83. doi:10.3847/1538-4357/aad0ef

Gopalswamy, N., and Kundu, M. R. (1987). Simultaneous radio and white light observations of the 1984 June 27 coronal mass ejection event. *Sol. Phys.* 114, 347–362. doi:10.1007/BF00167350

Gopalswamy, N., Nitta, N., Akiyama, S., Mäkelä, P., and Yashiro, S. (2012). Coronal magnetic field measurement from EUV images made by the solar dynamics observatory. *Astrophys. J.* 744, 72. doi:10.1088/0004-637X/744/1/72

Helmboldt, J. F., Clarke, T. E., and Kassim, N. E. (2022). Remote sensing of mid-latitude ionospheric magnetic field fluctuations using cosmic radio sources. *Radio Sci.* 57, e07372. doi:10.1029/2021RS007372

Helmboldt, J. F., and Kassim, N. E. (2009). The evolution of Cassiopeia A at low radio frequencies. *Astron. J.* 138, 838–844. doi:10.1088/0004-6256/138/3/838

Helmboldt, J. F., Markowski, B. B., Bonanno, D. J., Clarke, T. E., Dowell, J., Hicks, B. C., et al. (2021). The deployable low-band ionosphere and transient experiment. *Radio Sci.* 56, e07298. doi:10.1029/2021RS007298

Helmboldt, J. F., and Zabotin, N. (2022). An observed trend between mid-latitudes km-scale irregularities and medium-scale traveling ionospheric disturbances. *Radio Sci.* 57, e07396. doi:10.1029/2021RS007396

Hicks, B. C., Paravastu-Dalal, N., Stewart, K. P., Erickson, W. C., Ray, P. S., Kassim, N. E., et al. (2012). A wide-band, active antenna system for long wavelength radio astronomy. *Publ. Astron. Soc. Pac.* 124, 1090–1104. doi:10.1086/668121

Kassim, N. E., Lazio, T. J. W., Erickson, W. C., Perley, R. A., Cotton, W. D., Greisen, E. W., et al. (2007). The 74 MHz system on the very large array. *Astrophys. J. Suppl. Ser.* 172, 686–719. doi:10.1086/519022

Klein, K.-L. (2021). Radio astronomical tools for the study of solar energetic particles I. Correlations and diagnostics of impulsive acceleration and particle propagation. *Front. Astron. Space Sci.* 7, 105. doi:10.3389/fspas.2020.580436

Kumari, A., Ramesh, R., Kathiravan, C., and Wang, T. J. (2017). Strength of the solar coronal magnetic field - a comparison of independent estimates using contemporaneous radio and white-light observations. *Sol. Phys.* 292, 161. doi:10.1007/s11207-017-1180-6

Law, C. J., and Bower, G. C. (2012). All transients, all the time: Real-time radio transient detection with interferometric closure quantities. *Astrophys. J.* 749, 143. doi:10.1088/0004-637X/749/2/143

Lemen, J. R., Title, A. M., Akin, D. J., Boerner, P. F., Chou, C., Drake, J. F., et al. (2012). The atmospheric imaging assembly (AIA) on the solar dynamics observatory (SDO). *Sol. Phys.* 275, 17–40. doi:10.1007/s11207-011-9776-8

Li, W., Pober, J. C., Hazelton, B. J., Barry, N., Morales, M. F., Sullivan, I., et al. (2018). Comparing redundant and sky-model-based interferometric calibration: A first look with phase II of the MWA. *Astrophys. J.* 863, 170. doi:10.3847/1538-4357/aad3c3

Mahrous, A., Alielden, K., Vršnak, B., and Youssef, M. (2018). Type II solar radio burst band-splitting: Measure of coronal magnetic field strength. *J. Atmos. Sol. Terr. Phys.* 172, 75–82. doi:10.1016/j.jastp.2018.03.018

McCauley, P. I., Cairns, I. H., Morgan, J., Gibson, S. E., Harding, J. C., Lonsdale, C., et al. (2017). Type III solar radio burst source region splitting due to a quasi-separatrix layer. *Astrophys. J.* 851, 151. doi:10.3847/1538-4357/aa9cee

McConnell, D. (1983). Evidence for arc sec radio burst sources in the upper corona. *Sol. Phys.* 84, 361–369. doi:10.1007/BF00157468

Miteva, R., Samwel, S. W., and Zabunov, S. (2022). Solar radio bursts associated with *in situ* detected energetic electrons in solar cycles 23 and 24. *Universe* 8, 275. doi:10.3390/universe8050275

Mondal, S., Oberoi, D., and Vourlidas, A. (2020). Estimation of the physical parameters of a CME at high coronal heights using low-frequency radio observations. *Astrophys. J.* 893, 28. doi:10.3847/1538-4357/ab7fab

Morosan, D. E., Gallagher, P. T., Zucca, P., O'Flannagain, A., Fallows, R., Reid, H., et al. (2015). LOFAR tied-array imaging and spectroscopy of solar S bursts. *Astron. Astrophys.* 580, A65. doi:10.1051/0004-6361/201526064

Payne-Scott, R., Yabsley, D. E., and Bolton, J. G. (1947). Relative times of arrival of bursts of solar noise on different radio frequencies. *Nature* 160, 256–257. doi:10.1038/160256b0

Perley, R. A., Chandler, C. J., Butler, B. J., and Wrobel, J. M. (2011). The expanded very large array: A new telescope for new science. *Astrophys. J.* 739, L1. doi:10.1088/2041-8205/739/1/L1

Pesnell, W. D., Thompson, B. J., and Chamberlin, P. C. (2012). The solar dynamics observatory (SDO). *Sol. Phys.* 275, 3–15. doi:10.1007/s11207-011-9841-3

Reid, H. A. S. (2020). A review of recent solar type III imaging spectroscopy. *Front. Astron. Space Sci.* 7, 56. doi:10.3389/fspas.2020.00056

Sasikumar Raja, K., Ramesh, R., Hariharan, K., Kathiravan, C., and Wang, T. J. (2014). An estimate of the magnetic field strength associated with a solar coronal mass ejection from low frequency radio observations. *Astrophys. J.* 796, 56. doi:10.1088/0004-637X/796/1/56

Seaton, D. B., West, M. J., Caspi, A., DeForest, C. E., Golub, L., Mason, J., et al. (2020). A strategy for a coherent and comprehensive basis for understanding the middle corona. *Zenodo*. doi:10.5281/zenodo.4025420

Taylor, G. B., Ellingson, S. W., Kassim, N. E., Craig, J., Dowell, J., Wolfe, C. N., et al. (2012). First light for the first station of the long wavelength Array. *J. Astron. Instrum.* 1, 1250004–1250284. doi:10.1142/S2251171712500043

van Haarlem, M. P., Wise, M. W., Gunst, A. W., Heald, G., McKean, J. P., Hessels, J. W. T., et al. (2013). LOFAR: The LOw-Frequency ARray. *Astron. Astrophys.* 556, A2. doi:10.1051/0004-6361/201220873

Vourlidas, A., Carley, E. P., and Vilmer, N. (2020). Radio observations of coronal mass ejections: Space weather aspects. *Front. Astron. Space Sci.* 7, 43. doi:10.3389/fspas.2020.00043

Vourlidas, A. (2004). "Radio observations of coronal mass Ejection4," in *Astrophysics and space science library. Vol. 314 of astrophysics and space science library*. Editors D. E. Gary, and C. U. Keller, 223. doi:10.1007/1-4020-2814-8_11

Vršnak, B., Magdalenić, J., and Zlobec, P. (2004). Band-splitting of coronal and interplanetary type II bursts. III. Physical conditions in the upper corona and interplanetary space. *Astron. Astrophys.* 413, 753–763. doi:10.1051/0004-6361:20034060

West, M. J., Seaton, D. B., Alzate, N., Caspi, A., DeForest, C. E., Gilly, C. R., et al. (2022). "A strategy for a coherent and comprehensive basis for understanding the middle corona," in *Heliophysics 2050: Measurements and technologies workshop*, 4060.

Wild, J. P., and McCready, L. L. (1950). Observatioas of the spectrum of high-intensity solar radiation at metre wavelengths. I. The apparatus and spectral types of solar burst observed. *Aust. J. Chem.* 3, 387. doi:10.1071/CH9500387

Wild, J. P., Smerd, S. F., and Weiss, A. A. (1963). Solar bursts. *Annu. Rev. Astron. Astrophys.* 1, 291–366. doi:10.1146/annurev.aa.01.090163.001451

Yan, Y., Chen, L., and Yu, S. (2016). "First radio burst imaging observation from Mingantu Ultrawide spectral Radioheliograph," in *Solar and stellar flares and their effects on planets*. Editors A. G. Kosovichev, S. L. Hawley, and P. Heinzel, Vol. 320, 427–435. doi:10.1017/S174392131600051X